Congenital Heart Disease

Tech Science Press

DOI: 10.32604/chd.2023.030312

ARTICLE

Comparison of 2D and 4D Flow MRI Measurements for Hemodynamic Evaluation of the Fontan Palliation

Elisa Listo[1,#], Nicola Martini[2,#], Stefano Salvadori[3], Elisa Valenti[3], Nicola Stagnaro[1], Gianluca Trocchio[4], Chiara Marrone[5], Alberto Clemente[6], Francesca Raimondi[7,*], Pierluigi Festa[5] and Lamia Ait Ali[5,8,*]

[1]Department of Radiology, IRCCS Istituto Giannina Gaslini, Genova, Italy

[2]U.O.C. Bioingegneria, Gabriele Monasterio CNR-Tuscany Foundation, Pisa, Italy

[3]Institute of Clinical Physiology CNR, Pisa, Italy

[4]Cardiology Unit, IRCCS Istituto Giannina Gaslini, Genova, Italy

[5]Pediatric Cardiology and GUCH Unit Massa, Gabriele Monasterio CNR-Tuscany Foundation, Massa, Italy

[6]Gabriele Monasterio CNR-Tuscany Foundation, Pisa, Italy

[7]Department of Cardiology, Azienda Ospedaliero-Universitaria Meyer, Florence, Italy

[8]Institute of Clinical Physiology CNR, Massa, Italy

[*]Corresponding Authors: Francesca Raimondi. Email: francesca.raimondi@meyer.it; Lamia Ait Ali. Email: aitlamia@ifc.cnr.it

[#]Elisa Listo and Nicola Martini contributed equally to the study

Received: 30 March 2023 Accepted: 10 August 2023 Published: 19 January 2024

ABSTRACT

Background: The assessment of Fontan circuit's flow is traditionally evaluated by multiple through-plane phase-contrast MRI acquisitions (2D flow), while recently, a single volumetric 4D-flow MRI acquisition is emerging as a comprehensive tool for the hemodynamic evaluation in congenital heart diseases. **Purpose:** To compare 2D and 4D-flow MRI measurements in patients after Fontan palliation and to evaluate parameters affecting potential disagreement. **Methods:** 39 patients after Fontan palliation (23 males, age 22 ± 11 years) who underwent cardiac MRI with 2D and 4D-flow MRI acquisition were included in the study. In all patients, blood flow quantification in the Fontan circuit and aorta by 2D flow and by 4D flow MRI acquisition blinding to the 2D results was performed. The agreement between 2D and 4D-flow MRI was calculated as the intraclass correlation coefficient (ICC). The mean absolute differences between 4D and 2D flows were analyzed using linear regression models. **Results:** 4D-flow MRI acquisition time was slightly lower than 2D (7.6 ± 1.8 min *vs.* 9.4 ± 3.3 min, $p = 0.03$). Flow was slightly predominant in the right pulmonary artery (58% of total pulmonary flow). Conduit/tunnel-pulmonary arteries flow accounted for 60% of the Fontan circuit. Agreement between 2D and 4D was overall good-to-excellent from ICC: 0.817 95% CI: 0.637–0.907 to 0.932 95% CI: 0.866–0.965. There was no significant influence of evaluated parameters on the agreement on 4D and 2D flow. **Conclusions:** 4D-flow MRI represents a valid tool in Fontan's flow quantification. Further larger studies are needed to confirm our results and to evaluate the impact of advanced 4D-flow MRI parameters on the prognostic stratification in patients after Fontan palliation.

KEYWORDS

Fontan palliation; fontan flows; 4D flow MRI; 2D flow MRI; cardiac magnetic resonance

1 Introduction

Fontan intervention is a palliative procedure that allows patients with a functionally single ventricle to reach adulthood. Although this type of surgical palliation has been performed for 50 years, its physiopathology is far from being clear, and many issues are still debated [1].

In fact, although all patients have basically the same abnormal circulation based on a total cavo-pulmonary connection, the Fontan system's failure may occur with great variability in timing and presentation, dictated by factors that are still not fully understood [2].

Cardiac Magnetic Resonance Imaging (cardiac MRI) has emerged as a useful non-invasive tool in the evaluation of complex congenital heart disease, and it represents now the gold standard for the quantification of volumes and ventricular function, for the study of heart and vessel morphology and for the quantification of valve flows [2–4], all key aspects in the follow-up of these patients.

One of the most important goals of cardiac MRI in patients after Fontan palliation is the evaluation of the venous and pulmonary circuit by assessing flow distribution in pulmonary branches, pulmonary veins, distribution of inferior and superior vena cava flows toward the pulmonary arteries, evaluation of aorto-pulmonary and venous collaterals [5]. A comprehensive hemodynamic evaluation of the Fontan circuit is crucial to better understanding the underlying pathophysiological mechanisms that contribute to the long-term outcome of these patients.

Traditionally, flow evaluation has always been assessed by 2D phase-contrast MRI sequences (2D flow). However, in recent years a volumetric acquisition called 4D flow MRI (4D: 3D+time) has emerged as an accurate and comprehensive technique [6] for the flow evaluation. As a matter of fact, 4D flow MRI allows a retrospective evaluation of flow volumes and velocities at any site of the acquired volume [7–10].

In 2D flow, the placement of the acquisition plane remains challenging and can lead to the underestimation of flow velocities if misplaced or not orthogonal to the flow of interest. In contrast, 4D flow MRI allows the acquisition of the entire thoracic volume, thus making this technique less operator-dependent and providing a retrospective calculation of flow volumes and velocities of any site of the acquired volume. Additionally, the recent technological advances in the pulse sequence/reconstruction allow a significant acceleration [11], all factors that can increase the reproducibility of the examination. However, 4D flow MRI is still not routinely used in clinical practice.

The aim of this study was to compare 2D and 4D flow MRI techniques in patients after Fontan palliation and to evaluate whether some patients' parameters could somehow influence the potential mismatch between 2D and 4D flow MRI.

2 Materials and Methods

2.1 Population Study

All consecutive patients with Fontan palliation who underwent cardiac MRI with 2D and 4D flow MRI acquisition between February 2018 and July 2021 were included in the study. Exclusion criteria were presence of non-diagnostic 2D or 4D flow sequences. The institutional review board approved the study.

Surgical history and clinical data were abstracted from the hospital records: gender, age at MRI, diagnosis, age at Glenn anastomosis if appropriate, age and type of Fontan intervention, length of follow-up after Fontan palliation. The last echocardiogram report was also reported for the evaluation of the degree of atrio-ventricular valves regurgitation.

2.2 Cardiac MRI

A 1.5 Tesla scanner (Signa Artist, GE Healthcare) and 3 Tesla scanner (Ingenia, Philips Healthcare) were used. A comprehensive MRI evaluation was performed following an examination protocol previously published [12].

Briefly, functionally single-ventricle short axis was visualized from the base to the apex, using a cardiac cine balanced steady-state free-precession (SSFP) pulse sequence with the following parameters: retrospective ECG gating, field of view 340–360 mm, flip angle 35°–50°, TE 1.4–1.9 ms, TR 2.8–3.8 ms, slice thickness 6–8 mm, slice gap 0 mm, number of signal averages 1–3, reconstructed cardiac phases 30. Several 2D flow scans were performed to evaluate the blood flow in the ascending aorta (Ao), the superior vena cava (SVC), the right pulmonary artery (RPA) and left pulmonary artery (LPA), the individual right and left pulmonary veins (PVs) and the inferior vena cava-pulmonary arteries-conduit/tunnel (abbreviated in the following by IVC-PA conduit) (Fig. 1). The following parameters were used for 2D flow acquisitions: field of view 280–340 mm, flip angle 15°–20°, slice thickness 5–6 mm, view per segment 1–2, number of signal averages 2–4, velocity-encoding (VENC) values 100–450 cm/s depending on the expected blood velocity, reconstructed cardiac phases 30. All 2D flow scans were acquired during free-breathing. The MRI study was completed using a contrast-enhanced (gadopentetate dimeglumine 0.2–0.4 ml/kg). MR angiographic sequence or a time-resolved angiography for the anatomic evaluation of the Fontan pathway. In patients aged <8 years or with incapacity to collaborate the CMR exam was performed on deep sedation using titrated propofol.

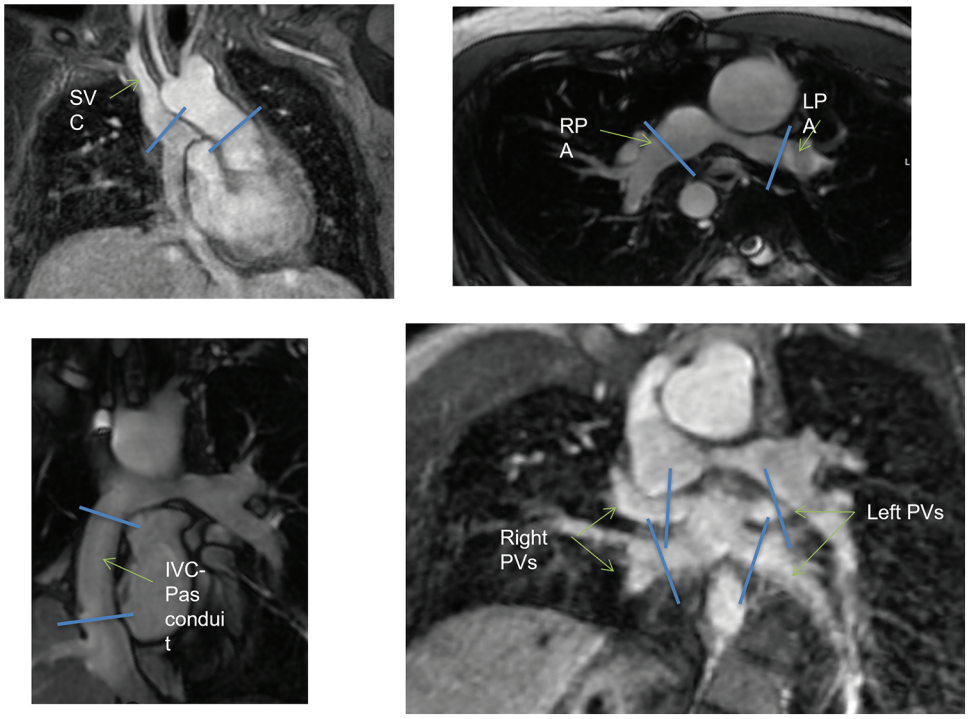

Figure 1: Schematic illustration of multiple 2D flow prescriptions. IVC, inferior vena cava; LPA, left pulmonary artery; RPA, right pulmonary artery; PA, pulmonary arteries; PVs, pulmonary veins; SVC, superior vena cava

A 4D flow MRI sequence was also prescribed in axial or coronal orientation covering the entire thorax with the following parameters: field of view 250–400 mm, flip angle 8°–15°, TR 3.8–5.3 ms, TE 2.0–3.2 ms,

slice thickness 2.2–3.0 mm, in-plane resolution 1.9–3.1 mm, view per segment 1–4, number of signal averages 1–4, VENC 70–150 cm/s, reconstructed cardiac phases 20–32, acquisition time 5–12 min. The SSFP and 2D flow images were elaborated by means of a commercially available software (Mass plus and CV Flow, respectively; version 4.0, MR Analytical Software Systems, Leiden, The Netherlands). Ventricular volumes, mass (indexed to body surface area) and the ejection fraction were calculated. 4D flow MRI data were processed using Arterys Cardio AIMR (Arterys Inc., San Francisco, CA). Examples of the 4D flow MRI are illustrated in Fig. 2 and Supplementary Movie S1.

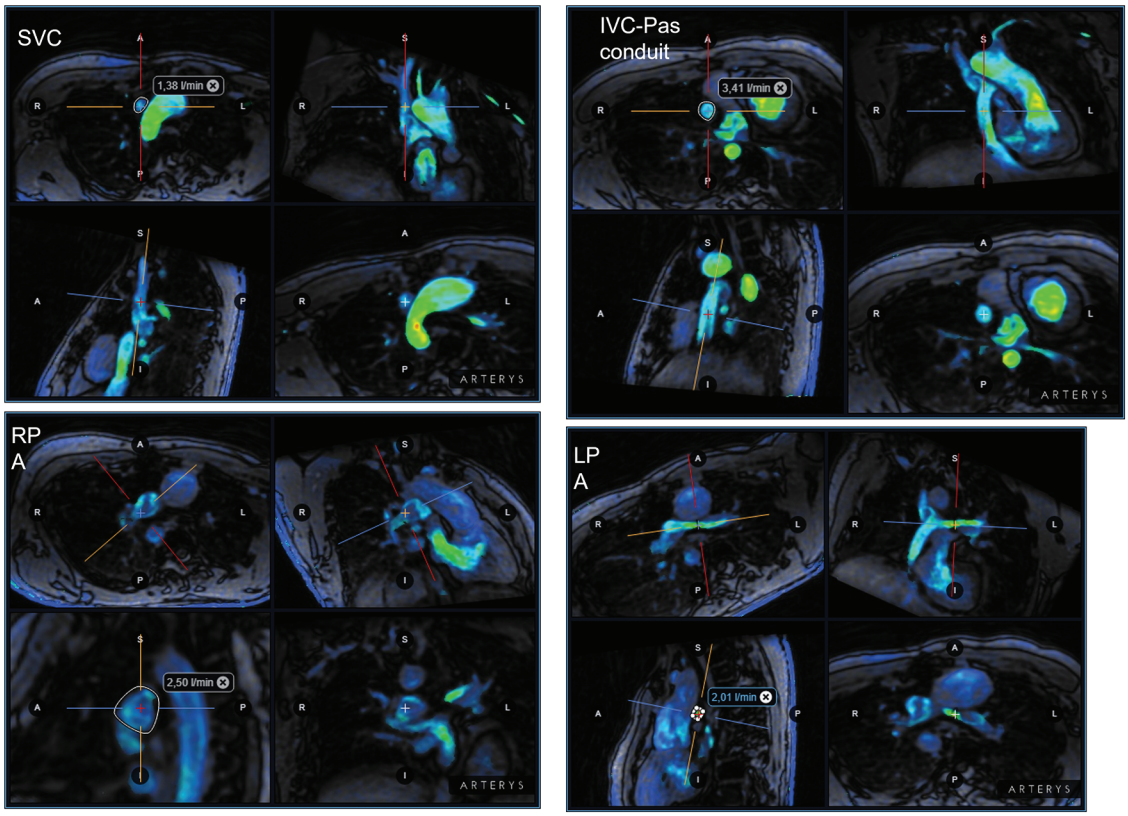

Figure 2: Examples of 4D flow MRI of the IVC-PA conduit in the same patient of Fig. 1. IVC, inferior vena cava; LPA, left pulmonary artery; RPA, right pulmonary artery; PA, pulmonary arteries; PVs, pulmonary veins; SVC, superior vena cava

Blood flow quantification was performed by reformatting 4D flow MRI data in all Fontan circuit flow by an investigator with more than 10 years' expertise blinded to the 2D flow results. A second investigator with 2 years' expertise in cardiac MRI in CHD evaluated a set of 21 4D flow acquisitions blinded to the 2D and previous 4D flow results.

Pulmonary arteries and Fontan conduit diameters were measured in axial and latero-lateral planes using multiplanar reformatting of volumetric 3D SSFP in the diastolic phase. The angle between pulmonary arteries and IVC-PA conduit was also calculated. Systemic-pulmonary collateral flows (QSPCs) was calculated as: (left pulmonary veins flow + right pulmonary veins flow) − (right pulmonary artery flow + left pulmonary artery flow) [13]. Values were normalized to body surface area. Effective cardiac index (CI) was calculated as (QAo flow-QSPCs)/BSA [14].

2.3 Statistical Analysis

Continuous variables were expressed as mean ± standard deviation (SD) or median (interquartile range IQR: 25th; 75th percentiles) if skewed. Categorical variables were expressed as percentage.

The correlation between continuous variables was tested with Pearson's correlation r coefficient or Spearman when indicated. Student's Independent *t*-test or Wilcoxon test were used as appropriate to compare continuous and variable differences. The agreement between 2D and 4D flow in the evaluation of each arterial and venous vessels for the evaluation of Fontan circuit was calculated using the intraclass correlation coefficient (ICC), computed by using a 2-way mixed model with measures of absolute agreement. Also, the intra-observer agreement and the inter-observer agreement of the 4D flow MRI was calculated in the same way, using the ICC. ICC data were interpreted using the following criteria: values between 0.5 and 0.75 indicate moderate agreement; 0.75 to 0.9 indicates good agreement; and >0.9 indicates excellent agreement [15]. For each ICC, the 95% confidence interval (CI) was calculated.

The mean absolute differences between 4D and 2D flows were analyzed using linear regression models, adjusted for age and gender. We also analyzed the influence of the following variables on the difference between 2D and 4D flow: scanner type, BSA, ventricle type, age at Fontan, RPA stenosis/hypoplasia, pulmonary arteries and conduit diameter, angle between conduit and RPA, angle between conduit and LPA, heart rate, oxygen saturation. For all analyses, age and gender were used as cofactors.

All statistical analyses were performed using SPSS (version 21.0).

3 Results

3.1 Patients Characteristics

From February 2018 to July 2021, 39 consecutive patients (25 males (64%) mean age 22 ± 11.4 years) underwent 41 CMR studies with 2D and 4D flow evaluation, 27 (65,8%) with a 1.5T scan and 14 (34,2%) with a 3T scan. Two patients underwent 2 examinations during the study period, in one case to confirm the result of percutaneous left pulmonary stent angioplasty, in the other one MRI was performed before and after artero-pulmonary percutaneous fistula occlusion.

Clinical and surgical data are summarized in Table 1. The most frequent diagnosis in our population was complex two ventricles (as defined in Table 1) in 23% followed by tricuspid atresia and atrio-ventricular canal and isomerism in 18%. The single ventricle was morphologically left in almost half of our population (51%). Glenn anastomosis was performed in 87% of patients before the Fontan procedure. Median age at Fontan procedure was 5.3 (3.7–8) years.

Table 1: Population demographic, history, and clinical data

	n = 39
Age at MRI (years)	22 ± 11.4
Male gender n (%)	25 (64)
Weight (kg)	52 ± 17.2
Height (cm)	163 (148, 170)
Body surface area (m^2)	1.5 ± 0.3
Diagnosis:	
Tricuspid atresia n (%)	7 (17.9)
Double inlet left ventricle n (%)	6 (15.4)

(Continued)

Table 1 (continued)

	n = 39
Complex 2 ventricles n (%) *	9 (23.1)
Hypoplastic left heart syndrome n (%)	4 (10.3)
Complex Atrio-Ventricular canal n (%)	7 (17.9)
Pulmonary atresia intact ventricular septum n (%)	3 (7.7)
Ebstein anomaly n (%)	1 (2.6)
Mitral atresia n (%)	2 (5.1)
Ventricle type:	
Two ventricles n (%)	7 (17.9)
Left ventricle n (%)	20 (51.3)
Right ventricle n (%)	12 (30.8)
Glenn n (%)	34 (87.2)
Age at Fontan (years) n = 37	5.3 (3.7, 8)
Fontan type:	1 (2.6)
Atrio-pulmonary n (%)	32 (82.1)
Extracardiac Conduit n (%)	1 (2.6)
Intracardiac Conduit n (%)	1 (2.6)
Intra-extracardiac Conduit n (%)	4 (10.3)
Lateral tunnel n (%)	
Fenestrated	14 (35.9)
Oxygen saturation (%)	94 (91, 97)

Note: *Criss cross heart in 4 patients, complex corrected transposition of great arteries and pulmonary atresia in 3 patients, malposition of the great arteries with complex ventricular septal defect in one patient, double inlet right ventricle and pulmonary atresia in one patient. Continuous variables are expressed as mean ± standard deviation or median and 25°; 75° percentiles.

The most common type of Fontan was extra-cardiac one in 82% (N = 36) of the population patients, Fenestration was performed in 14 (36%) of patients but only 5 of them had the fenestration still present at the time of the study. Mean follow-up after Fontan procedure was 14.4 ± 9.7 years.

3.2 Cardiac MRI

Cardiac MRI characteristics of the population study are reported in Table 2. In summary, the median indexed end-diastolic volume was 95 (78–119) ml/m^2 with a mean ejection fraction (EF) of 53.3 ± 11.4%. Cardiac index was 2.9 ± 0.5 l/min/m^2. Flow was slightly higher in RPA than in LPA (respectively 1.3 ± 0.4 l/min/m^2 *vs.* 1.0 ± 0.3 l/min/m^2, p = 0.039 in 2D flow and 1.2 ± 0.5 l/min/m^2 *vs.* 0.9 ± 0.4 l/min/m^2, p = 0.039 in 4D flow) (Fig. 3), As well as the flow, axial and latero-lateral diameters were slightly higher in RPA than LPA (RPA l4.8 ± 4.2 × 15.1 ± 4.2 mm *vs.* LPA 12.2 ± 3.2 × 12.6 ± 3.4 mm, p = 0.001). Moreover, RP was hypoplastic in 5 (13%) patients and LPA in 9 patients 9 (23%). RSVC flow accounted for 40% of the Fontan circuit whereas IVC-PA conduit flow accounted for 60% of total pulmonary flow. Mean aorto-pulmonary collaterals accounted for 0.8 l ± 0.7 l/min/m^2 (24% of CI).

3.3 Comparison between the 2D and 4D Flow

It was possible to calculate 2D flow and 4D flow in the entire Fontan circuit in almost all patients (n = 35). Only the RPA in one patient and pulmonary veins in 4 patients could not be measured. In one examination it was not possible to calculate accurately all arterial and venous flows in the 4D flow

acquisition because of excessive breathing and movement artifacts. Second reader was not able to evaluate the RPA flow in one patient.

Table 2: Cardiac MRI findings

End diastolic ventricular volume (ml/m^2)	95 (78, 119)
End systolic ventricular volume (ml/m^2)	46 (32, 58)
Ventricular ejection fraction (%)	53.3 ± 11.4
Ventricle mass	63 (49.7, 75.5)
Mass/volume	0.6 ± 0.1
IVC-PA conduit 4D flow (l/min/m^2)	1.3 ± 0.5
IVC-PA conduit 2D flow (l/min/m^2)	1.5 ± 0.6
SVC 4D flow (l/min/m^2)	1 ± 0.3
SVC 2D flow (l/min/m^2)	0.9 (0.7, 1.2)
CI 4D flow (l/min/m^2)	2.9 ± 0.7
CI 2D flow (l/min/m^2)	3.0 ± 0.7
RPA 4D flow (l/min/m^2)	1.2 ± 0.5
RPA 2D flow (l/min/m^2)	1.3 ± 0.4
LPA 4D flow (l/min/m^2)	0.9 ± 0.4
LPA 2D flow (l/min/m^2)	1.0 ± 0.3
Right PVs 4D flow (l/min/m^2)	1.5 ± 0.4
Right PVs 2D flow (l/min/m^2)	1.7 ± 0.6
Left PVs 4D flow (l/min/m^2)	1.3 ± 0.4
Left PVs 2D flow (l/min/m^2)	1.4 ± 0.4
AOC 4D flow (l/min/m^2)	0.6 ± 0.5
AOC 2D flow (l/min/m^2)	0.8 ± 0.7
LPA diameter (axial) (mm)	12.2 ± 3.2
LPA diameter (latero-lateral) (mm)	12.6 ± 3.4
LPA stenosis/hypoplasia n (%)	9 (23.1%)
RPA diameter (axial) (mm)	14.8 ± 4.2
RPA diameter (latero-lateral) (mm)	15.1 ± 4.2
RPA stenosis/hypoplasia n (%)	5 (12.8%)

The acquisition time of the 4D flow was lower than the whole 2D flow acquisition (4D *vs.* 2D: 7.6 ± 1.8 min *vs.* 9.4 ± 3.3 min, $p = 0.03$).

The acquisition time of 4D flow was not affected by the type of scanners (1.5T *vs.* 3.0T: 7.8 ± 1.7 min *vs.* 7.0 ± 1.9 min, $p = 0.054$, corrected by age and heart rate).

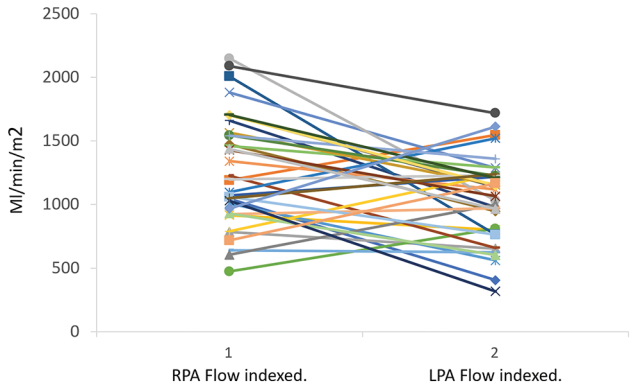

Figure 3: Pulmonary flow distribution calculated by 2D flow. LPA, left pulmonary artery; RPA, right pulmonary artery

HR variability among 2D flow acquisitions was low (1.82 ± 0.99 bpm) and there was no significant difference between the average value of the heart rate compared to 4D flow HR (−2, 1.75).

The agreement between 2D and 4D flow measurements is reported in Table 3. Differences between 4D and 2D flow volumes ranged from −0.31 l/min to 0.01 l/min with a little underestimation of 4D flow evaluation in comparison with the 2D flow assessment. Agreement between 2D and 4D was overall good-to-excellent from ICC: 0.817 95% CI: 0.637–0.907 for the right pulmonary vein flows to 0.932 95% CI: 0.866–0.965 for the SVC flow (Table 3).

Table 3: Agreement between 4D and 2D flow measurements

	Flow difference 4D–2D [l/min]			Intraclass correlation		
Vessel	Mean	Median	Standard deviation	ICC	95% CI lower limit	95% CI upper limit
IVC-PA conduit	−0.26	−0.24	0.58	0.904	0.811	0.951
SVC	0.01	0.04	0.27	0.932	0.866	0.965
Ao	−0.28	−0.20	0.58	0.926	0.855	0.962
RPA	−0.06	−0.08	0.48	0.868	0.747	0.932
LPA	−0.17	−0.15	0.33	0.932	0.869	0.964
Right PVs	−0.31	−0.30	0.65	0.817	0.637	0.907
Left PVs	−0.18	−0.19	0.38	0.917	0.832	0.959

Note: IVC, inferior vena cava; PA, pulmonary artery; SVC, superior vena cava; LPA, left pulmonary artery; RPA, right pulmonary artery; Ao, aorta; PVs, pulmonary veins.

The intra-observer agreement of the 4D flow calculation was excellent as well as inter-observer evaluation (Table 4). The agreement between the sum of systemic flows (IVC-PA conduit + SVC flow 2D) and pulmonary arteries flow (LPA Flow + RPA flow) assessed by 2D and 4D flow was excellent (2D flow: ICC 0.936 95% CI: 0.871–0.969; 4D flow: ICC 0.951 95% CI: 0.901–0.976).

The agreement between aortic flow and the sum of PVs (Left PVs flow + Right PVs flow) in patients without fenestration and /or collateral vessels (n = 24) was good for the 2D flow and excellent for the 4D flow (2D flow: ICC 0.897 95% CI: 0.762–0.956; 4D flow: ICC 0.966 95% CI: 0.921–0.985).

Table 4: Intra-observer and inter-observer agreement of 4D flow

	Intra-observer agreement			Inter-observer agreement		
Vessel	ICC	95% CI lower limit	95% CI upper limit	ICC	95% CI lower limit	95% CI upper limit
IVC-PA conduit	0.973	0.948	0.986	0.980	0.950	0.992
SV	0.966	0.934	0.983	0.971	0.930	0.988
Ao	0.984	0.970	0.992	0.971	0.929	0.988
RPA	0.927	0.860	0.962	0.941	0.847	0.977
LPA	0.958	0.916	0.979	0.932	0.833	0.972
Right PVs	0.912	0.831	0.954	0.966	0.915	0.986
Left PVs	0.932	0.867	0.965	0.954	0.883	0.982

Note: IVC, inferior vena cava; PA, pulmonary artery; SVC, superior vena cava; LPA, left pulmonary artery; RPA, right pulmonary artery; Ao, aorta; PVs, pulmonary veins.

3.4 Influence of Anatomical and Functional Data on the Agreement between 2D and 4D Flow Quantification

No significant influence of the considered variables (scanner type, BSA, ventricle type, age at Fontan, RPA stenosis/hypoplasia, pulmonary arteries and conduit diameter, angle between conduit and RPA, angle between conduit and LPA, heart rate, oxygen saturation) on the agreement on 4D and 2D flow evaluation was found. The results of this analysis are reported in Supplementary Table S1.

4 Discussion

In this study, we evaluated the agreement of the arterial and venous flows calculated by 4D flow and 2D flow sequences in a relatively large population of functionally single ventricles after Fontan palliation.

Cardiac MRI is nowadays a non-invasive imaging tool validated for the diagnosis and follow-up of patients with congenital heart disease [16] and it is recommended regularly in the follow-up of patients after Fontan Palliation [17] for the evaluation of ventricular volumes and function, Fontan circulation flows and their distribution [3,18] and for quantification of aorto-pulmonary and veno-venous collaterals [5,13,18]. Cardiac MRI is the gold standard for the evaluation of ventricular volumes and function [19] and is the only method that allows us to accurately quantify the flow in any venous or arterial district thanks to the commonly used 2D phase-contrast MRI technique [20,21]. Although the 2D flow phase contrast sequence is considered the gold standard in flow quantification [22], in recent years the development of the 4D flow volumetric sequence aroused much interest, especially for the evaluation of complex congenital heart disease. In contrast to standard 2D flow which allows the evaluation of blood flow in a single prescribed 2D slice, 4D flow MRI can provide information on the temporal and spatial evolution of 3D blood flow with full volumetric coverage of any cardiac or vascular region of interest [23,24]. Our study includes the evaluation of flow in the aorta, the pulmonary branches, the pulmonary veins, and the IVC-PA conduit, and this comprehensive evaluation is obviously time-consuming.

In our population, the distribution of the flow was slightly higher in the RPA (57%) and the contribution of IVC flow to total systemic venous return was 60% in line with data reported by Whitehead et al.'s study [25].

The overall acquisition time of the 2D flow sequence in our population was higher than the acquisition of the 4D flow MRI, even though we did not include the additional sequences often necessary for the accurate planning of 2D flow scans. Moreover, while the acquisition time of 4D flow was previously considered a limiting factor, the recent technological improvement of MRI technologies has significantly reduced this disadvantage.

We found an excellent agreement between the 2D and 4D flow sequences, in line with the results of previous studies [18]. The agreement was slightly lower for pulmonary veins with lower 2D flow compared to 4D flow data. One possible explanation is that with a 2D technique, the evaluation of all anatomical variants of pulmonary veins is challenging.

We have not found demographic, anatomical, or spatial factors that can influence the agreement between the two methods. Theoretically, heart rate variability between the multiple 2D flow sequences could be a limiting and altering factor, while in 4D flow acquisition, the heart rate is obviously the same for all analyzed planes.

4.1 Clinical Implication

Our data confirmed that the 4D flow sequence could be a valid alternative to the multiple 2D flow sequences in this population, allowing us to save time in an already complex and time-consuming examination. With already available accelerated 4D flow MRI sequences, 4D flow scan time is sensibly reduced. Finally, the 4D flow technique has proven to have low inter and intra-observer variability.

4.2 Limitations

One major limitation of our study is the use of two different scanners. However, the scanner type did not influence the agreement between the two techniques. Moreover, we did not test the influence of respiration on flow characteristics in the Fontan circulation

5 Conclusion

Our study confirms that the 4D flow MRI technique represents a valid alternative to Fontan's flow quantification. The intra- and inter-observer agreement was excellent, without any analyzed parameter capable of influencing this agreement. The reduced scan time of 4D flow acquisition, thanks to the recent advanced technologies and the possibility of a retrospective calculation of flow volumes and velocities at any site of the entire acquired volume, could help us to take a leap forward and progress in knowledge of this challenging circulation model. Larger studies are needed to confirm our results and to evaluate the differences in terms of field strength and vendor and also breathing phases in flow calculation in patients with Fontan circulation.

Acknowledgement: None.

Funding Statement: The authors received no specific funding for this study.

Author Contributions: EL: Conceptualization, Methodology, Writing-Original Draft. NM: Conceptualization, Methodology, Formal Analysis, Writing-Original Draft. SS and EV: Formal Analysis, Methodology, Writing-Original Draft. NS and GT: Conceptualization, Writing-Review & Editing. CM and AC: Investigation, Resources, Writing-Review & Editing. FR: Conceptualization, Writing-Review & Editing. LA: Conceptualization, Methodology, Writing-Original Draft. PF: Conceptualization, Methodology, Resources, Writing-Review & Editing.

Availability of Data and Materials: The datasets generated during and/or analyzed during the current study are available from the corresponding author on reasonable request.

Ethics Approval: The Institutional Review Board and Regional Committee (CEAVNO) approved the study (Study No. 13756 approved in September 2018).

Conflicts of Interest: The authors declare that they have no conflicts if interest to report regarding the present study.

Supplementary Materials: The supplementary materials are available online at https://doi.org/10.32604/chd.2023.030312.

References

1. Gewillig, M., Brown, S. C., Eyskens, B., Heying, R., Ganame, J. et al. (2010). The Fontan circulation: Who controls cardiac output? *Interactive Cardiovascular and Thoracic Surgery, 10(3),* 428–433. https://doi.org/10.1510/icvts.2009.218594
2. Khairy, P., Poirier, N., Mercier, L. A. (2007). Univentricular heart. *Circulation, 115(6),* 800–812. https://doi.org/10.1161/CIRCULATIONAHA.105.592378
3. Kilner, P. J., Geva, T., Kaemmerer, H., Trindade, P. T., Schwitter, J. et al. (2010). Recommendations for cardiovascular magnetic resonance in adults with congenital heart disease from the respective working groups of the European Society of Cardiology. *European Heart Journal, 31(7),* 794–805. https://doi.org/10.1093/eurheartj/ehp586
4. Rathod, R. H., Prakash, A., Kim, Y. Y., Germanakis, I. E., Powell, A. J. et al. (2014). Cardiac magnetic resonance parameters predict transplantation-free survival in patients with Fontan circulation. *Circulation: Cardiovascular Imaging, 7(3),* 502–509. https://doi.org/10.1161/CIRCIMAGING.113.001473
5. Raimondi, F., Martins, D., Coenen, R., Panaioli, E., Khraiche, D. et al. (2021). Prevalence of venovenous shunting and high-output state quantified with 4D Flow MRI in patients with Fontan circulation. *Radiology: Cardiothoracic Imaging, 3(6),* e210161. https://doi.org/10.1148/ryct.210161
6. Rijnberg, F. M., van Assen, H. C., Juffermans, J. F., Kroft, L. J. M., van den Boogaard, P. J., et al. (2021). Reduced scan time and superior image quality with 3D flow MRI compared to 4D flow MRI for hemodynamic evaluation of the Fontan pathway. *Scientific Reports, 11(1),* 6507. https://doi.org/10.1038/s41598-021-85936-6
7. Dyverfeldt, P., Bissell, M., Barker, A. J., Bolger, A. F., Carlhall, C. J. et al. (2015). 4D flow cardiovascular magnetic resonance consensus statement. *Journal of Cardiovascular Magnetic Resonance, 17(1),* 72. https://doi.org/10.1186/s12968-015-0174-5
8. Isorni, M. A., Moisson, L., Moussa, N. B., Monnot, S., Raimondi, F. et al. (2020). 4D flow cardiac magnetic resonance in children and adults with congenital heart disease: Clinical experience in a high volume center. *International Journal of Cardiology, 320,* 168–177. https://doi.org/10.1016/j.ijcard.2020.07.021
9. Isorni, M. A., Martins, D., Ben Moussa, N., Monnot, S., Boddaert, N. et al. (2020). 4D flow MRI versus conventional 2D for measuring pulmonary flow after Tetralogy of Fallot repair. *International Journal of Cardiology, 300(6),* 132–136. https://doi.org/10.1016/j.ijcard.2019.10.030
10. Soulat, G., Scott, M. B., Pathrose, A., Jarvis, K., Berhane, H. et al. (2022). 4D flow MRI derived aortic hemodynamics multi-year follow-up in repaired coarctation with bicuspid aortic valve. *Diagnostic and Interventional Imaging, 103(9),* 418–426. https://doi.org/10.1016/j.diii.2022.04.003
11. Valvano, G., Martini, N., Huber, A., Santelli, C., Binter, C. et al. (2017). Accelerating 4D flow MRI by exploiting low-rank matrix structure and hadamard sparsity. *Magnetic Resonance in Medicine, 78(4),* 1330–1341. https://doi.org/10.1002/mrm.26508
12. Ait-Ali, L., de Marchi, D., Lombardi, M., Scebba, L., Picano, E. et al. (2011). The role of cardiovascular magnetic resonance in candidates for Fontan operation: Proposal of a new algorithm. *Journal of Cardiovascular Magnetic Resonance, 13(1),* 69. https://doi.org/10.1186/1532-429X-13-69
13. Grosse-Wortmann, L., Al-Otay, A., Yoo, S. J. (2009). Aortopulmonary collaterals after bidirectional cavopulmonary connection or Fontan completion: Quantification with MRI. *Circulation: Cardiovascular Imaging, 2(3),* 219–225. https://doi.org/10.1161/CIRCIMAGING.108.834192
14. Ait Ali, L., Cadoni, A., Rossi, G., Keilberg, P., Passino, C. et al. (2017). Effective cardiac index and systemic-pulmonary collaterals evaluated by cardiac magnetic resonance late after fontan palliation. *American Journal of Cardiology, 119(12),* 2069–2072. https://doi.org/10.1016/j.amjcard.2017.03.040
15. Koo, T. K., Li, M. Y. (2016). A guideline of selecting and reporting intraclass correlation coefficients for reliability research. *Journal of Chiropractic Medicine, 15(2),* 155–163. https://doi.org/10.1016/j.jcm.2016.02.012

16. Ntsinjana, H. N., Hughes, M. L., Taylor, A. M. (2011). The role of cardiovascular magnetic resonance in pediatric congenital heart disease. *Journal of Cardiovascular Magnetic Resonance, 13(1),* 51. https://doi.org/10.1186/1532-429X-13-51
17. Rychik, J., Atz, A. M., Celermajer, D. S., Deal, B. J., Gatzoulis, M. A. et al. (2019). Evaluation and management of the child and adult with Fontan circulation: A scientific statement from the American Heart Association. *Circulation, 140(6),* e234–e284. https://doi.org/10.1161/CIR.0000000000000696
18. Valverde, I., Nordmeyer, S., Uribe, S., Greil, G., Berger, F. et al. (2012). Systemic-to-pulmonary collateral flow in patients with palliated univentricular heart physiology: Measurement using cardiovascular magnetic resonance 4D velocity acquisition. *Journal of Cardiovascular Magnetic Resonance, 14(1),* 25. https://doi.org/10.1186/1532-429X-14-25
19. Aquaro, GD., Camastra, G., Monti, L., Lombardi, M., Pepe, A. et al. (2017). Reference values of cardiac volumes, dimensions, and new functional parameters by MR: A multicenter, multivendor study. *Journal of Magnetic Resonance Imaging, 45(4),* 1055–1067. https://doi.org/10.1002/jmri.25450
20. Markl, M., Chan, F. P., Alley, M. T., Wedding, K. L., Draney, M. T. et al. (2003). Time-resolved three-dimensional phase-contrast MRI. *Journal of Magnetic Resonance Imaging, 17(4),* 499–506. https://doi.org/10.1002/(ISSN)1522-2586
21. Pelc, N. J., Herfkens, R. J., Shimakawa, A., Enzmann, D. R. (1991). Phase contrast cine magnetic resonance imaging. *Magnetic Resonance Quarterly, 7(4),* 229–254. https://www.ncbi.nlm.nih.gov/pubmed/1790111
22. Fratz, S., Chung, T., Greil, G. F., Samyn, M. M., Taylor, A. M. et al. (2013). Guidelines and protocols for cardiovascular magnetic resonance in children and adults with congenital heart disease: SCMR expert consensus group on congenital heart disease. *Journal of Cardiovascular Magnetic Resonance, 15(1),* 51. https://doi.org/10.1186/1532-429X-15-51
23. Stankovic, Z., Allen, B. D., Garcia, J., Jarvis, K. B., Markl, M. (2014). 4D flow imaging with MRI. *Cardiovascular Drugs and Therapy, 4(2),* 173–192. https://doi.org/10.3978/j.issn.2223-3652.2014.01.02
24. Roos, P. R., Rijnberg, F. M., Westenberg, J. J. M., Lamb, H. J. (2023). Particle tracing based on 4D flow magnetic resonance imaging: A systematic review into methods, applications, and current developments. *Journal of Magnetic Resonance Imaging, 57(5),* 1320–1339. https://doi.org/10.1002/jmri.28540
25. Whitehead, K. K., Sundareswaran, K. S., Parks, W. J., Harris, M. A., Yoganathan, A. P. et al. (2009). Blood flow distribution in a large series of patients having the Fontan operation: A cardiac magnetic resonance velocity mapping study. *The Journal of Thoracic and Cardiovascular Surgery, 138(1),* 96–102. https://doi.org/10.1016/j.jtcvs.2008.11.062